Int. J. Heat Mass Transfer. Vol. 33, No. 3, pp. 507–516, 1990
Printed in Great Britain

0017–9310/90 $3.00 + 0.00

A simplified model for radiative source term in combusting flows

S. BHATTACHARJEE

Mechanical and Nuclear Engineering Department, Mississippi State University, Mississippi State, MS 39762, U.S.A.

and

W. L. GROSSHANDLER

Department of Mechanical and Materials Engineering, Washington State University, Pullman, WA 99164-2920, U.S.A.

(*Received* 19 *December* 1988 *and in final form* 13 *June* 1989)

Abstract—An 'effective angle model' is proposed for evaluating the radiation source term in flows of non-isothermal absorbing/emitting media confined within rectangular and cylindrical ducts. While the model possesses the simplicity of two-flux schemes, it incorporates the influence of the enclosure geometry, and is particularly suitable for parabolic flows since the source term is based on the properties of the current marching station in the solution procedure. The model is first developed for two-dimensional geometry and applied to a test case of a gray medium reproducing analytical results within a few percent. It is next applied to a two-dimensional slot burner with radiation from fuel and products of combustion accounted for, and is shown to compare favorably with a detailed calculation of the source term. With some modification, the model is extended to a cylindrical gas-fired burner. A study of various parameters and different types of boundary conditions demonstrates the promise of the model.

INTRODUCTION

RADIATIVE heat transfer is often the most important means of energy transport in high temperature combustion systems. While the process is well described by the radiative transfer equation, analytical solutions are cumbersome because of a number of reasons. Notable among those are the multi-dimensional nature of the radiation process, spectral and temperature dependence of properties of the medium, turbulence–radiation interaction, soot formation and inhomogeneity of the medium. As a result, in the modeling of a turbulent combusting flow field, the additional burden of detailed radiation calculation often makes it imperative to use a very simplified model for radiation, or to neglect this important process altogether.

The simplest radiation model assumes the medium to be spectrally gray, homogeneous, and at an effective constant temperature. For non-gray gases, methods developed by Hottel [1] have been widely used. For non-isothermal, non-gray gases, narrow band models [2, 3] are the most accurate for determining radiation intensity along a line of sight; but they are also notoriously cumbersome. Wide band models [4, 5] are simpler to use but they still are complex. The sum of the gray gas model [6] is of similar complexity as the wide band models. The total transmittance non-homogeneous (TTNH) model [7, 8] is amongst the simplest of any models with an error of less than 15% when compared to narrow band results.

While these models simplify evaluation of intensity along a non-gray, non-isothermal line of sight, the multi-dimensional nature of radiation still poses a problem. For wall flux calculations, Hottel and Sarofim's mean-beam-length model [9] entirely eliminates directionally by replacing the radiating medium with an equivalent hemispherical enclosure. For calculating the radiation source term within the flow field, the two-flux model [10] is the simplest of all available models. Only two intensities are needed to be computed at any location. The more accurate methods, such as discrete ordinate [11] and the discrete transfer methods [12], are more complicated and three-dimensional in nature. In addition, use of these methods in parabolic flows destroys the marching nature of the solution procedure, as properties throughout the flow must be stored in order to calculate intensities in different directions.

The present model encompasses the advantages of both the mean-beam-length and two-flux models. In order to determine the radiative source term at a given location, only two intensities in two 'effective' directions are evaluated. The effective direction contains information about the geometry of the enclosure. These effective intensities are evaluated using the flow properties in the cross-stream direction, making the model ideal for parabolic flow calculations where the cross-stream properties are overwritten after every marching step.

In what follows, the model will be developed from the mean-beam-length idea for a two-dimensional

NOMENCLATURE

A	surface area [m^2]
a	total local absorption coefficient [m^{-1}]
B	point on the flame circle
b	distance of outer wall from axis [m]
c	distance of inner wall from axis [m]
C	arbitrary point outside the flame circle
D	separation between two planes, diameter [m]
i	total intensity [W m^{-2} sr^{-1}]
L	mean beam length [m]
L–L	plane containing the left face of the element
P	pressure [N m^{-2}]
q_r	radiative flux vector [W m^{-2}]
q_L	radiative flux in the y (or r) direction caused by the left hemisphere [W m^{-2}] (see equations (5) and (7))
R	radius [m]
r	radial position [m]
r_w	distance from wall [m]
T	temperature [K]
U	velocity [m s^{-1}]
V	volume [m]
W	width [m]
x, y	coordinates [m].

Greek symbols

β	angle between line of sight and normal to the surface
η	azimuthal angle
θ, ϕ	angles describing line of sight in cylindrical coordinates (see Fig. 10)
κ	optical thickness
σ	Stefan–Boltzmann constant [W m^{-2} K^{-4}]
ω	solid angle.

Subscripts

b	blackbody
D	over distance D
e	effective
i	incident, inner
L	left
o	outer
P	Planck
R	right
w	wall
1	left wall
2	right wall.

Superscripts

¯	average over solid angle
′	directional quantity.

parallel plate geometry. It is then compared with the available analytical solution for temperature and heat flux in a gray medium in radiative equilibrium between two parallel plates. Application of the simple model to a two-dimensional slot burner containing fuel, oxidizer, and products is then compared to a calculation of the radiant flux using a detailed geometric integration. After extending the model to cylindrical geometry, a similar evaluation is made in a cylindrical gas burner. The cylindrical model is further tested by applying it to the Graetz problem with radiation, for which results [13] are already available. Finally, the effects of different parameters and different types of boundary conditions on the applicability of this model are evaluated.

MODEL FOR PLANAR ENCLOSURE

The radiation source term, which is the net radiative influx at a given location, can be expressed as [14]

$$-\nabla \cdot q_r = 4\pi(a_i \bar{i}_i - a_p i_b). \quad (1)$$

If the Planck and mean incident absorption coefficients, a_p and a_i, are approximated by the local absorption coefficient then the only term that cannot be locally determined is the mean incident intensity $\bar{i}_i$. In fact, it is the evaluation of this mean intensity that brings in the three-dimensional nature of radiation. At any given location, the value of $\bar{i}_i$ depends on the intensity arriving from all possible lines of sight visible from this location. The effective angle model (EAM) described below simplifies the averaging procedure by picking only two appropriate directions.

Consider the control volume in a radiating medium between two isothermal parallel plates shown in Fig. 1. If the axial variation of properties is relatively small,

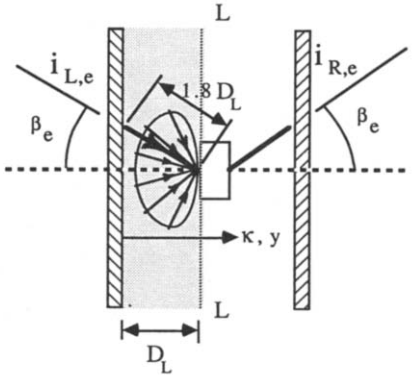

FIG. 1. Description of the effective angle β_e for parallel plate geometry.

the net radiative flux is stronger in the direction perpendicular to the axis. In studying the entrance region inside high temperature ducts several researchers [13, 15, 16] showed the insignificance of the axial flux. The average incident flux on the control surface of Fig. 1 is, thus, largely determined by the flux incident on its left and right faces

$$\bar{i}_i \approx \frac{\bar{i}_L + \bar{i}_R}{2}. \tag{2}$$

In the present model the average intensities incident on the left and right faces of the control volume of Fig. 1 are approximated by two special intensities, $i_{L,e}$ and $i_{R,e}$, respectively, coming from the two effective lines of sight.

For evaluating the effective direction for $i_{L,e}$, let us consider the dotted region between the left boundary wall and the imaginary plane L–L of Fig. 1. If the medium were isothermal and homogeneous, the mean-beam-length model would produce an accurate prediction of the heat flux incident on plane L–L. If D_L is the separation between the boundary wall and plane L–L, then the mean beam length for this configuration is $1.8D_L$ [14]. An intensity arriving at an angle $\beta_e = \cos^{-1}(1/1.8) = 56°$ with the normal to plane L–L will have the same path length as the mean beam, and, therefore, will represent the average intensity incident on plane L–L due to radiation from the dotted region. In a similar manner, the effective direction for $i_{R,e}$ can be shown to be 56° with the normal. Thus for a homogeneous, isothermal medium, the effective directions are found, and the problem of finding the radiative source term has reduced to determining the effective intensities $i_{L,e}$ and $i_{R,e}$.

With a bold assumption, this same direction is chosen as the effective direction for a non-isothermal, non-homogeneous medium. This approach was used in ref. [17] where very good agreement was obtained with more accurate calculations in evaluating radiative wall flux in planar and cylindrical enclosures containing radial variations in temperature and species concentration. In addition to radial variation, properties may change in the axial direction in a realistic combusting flow. A second assumption is now made to take care of the axial variation of properties. For a given location, the properties across the flow at that location are assumed to prevail at all other axial positions. Thus the effective intensities can be determined with properties at the local cross-stream position with only the path length extended by a factor of $1/\cos\beta_e$. If properties change monotonically along the axis, then the value of a property at the desired downstream position can be expected to be close to the mean value, obtained by averaging the property over nearby axial locations up to a distance of a few optical depths. A significant result of this assumption is the simplicity it achieves. As the properties of only the current downstream location are needed, the method becomes consistent with parabolic flow computations.

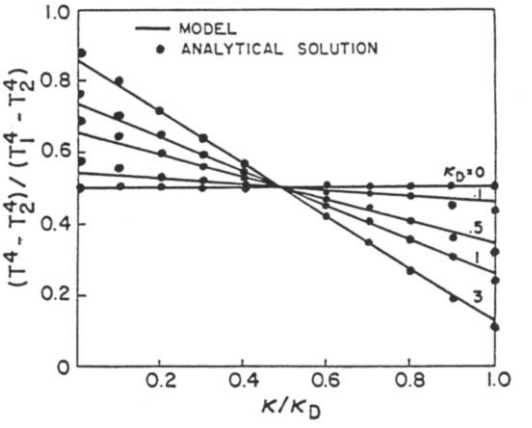

FIG. 2. Temperature distribution in a stagnant gray gas under radiative equilibrium between two black parallel plates. $T_1 = 2000$ K and $T_2 = 1000$ K.

These assumptions are challenged by subjecting the model to severe changes of properties in both axial and cross-stream directions, in the evaluation of the radiative source term in gas burners under different conditions. But first, the model has been applied to a case where an analytical solution is available.

TESTING THE PLANAR MODEL

Heaslet and Warming problem

The effective angle model has been employed to determine the temperature distribution in a stagnant gray gas between parallel plates kept at constant temperatures, a case for which Heaslet and Warming [18] produced an analytical solution. Applying the radiative equilibrium condition to equation (1) and substituting equation (2) for the mean incident intensity, one obtains

$$\bar{i} = \frac{\sigma T^4}{\pi} \approx \frac{\bar{i}_L + \bar{i}_R}{2} \approx \frac{i_{L,e} + i_{R,e}}{2}. \tag{3}$$

The effective intensities, $i_{L,e}$ and $i_{R,e}$, can be obtained by numerically integrating the radiative transfer equation if the temperature distribution with optical distance is supplied. The temperature distribution, being the desired unknown, is found by an iterative procedure in which, starting with a guessed temperature profile, equation (3) is used repeatedly to produce a converged solution. The convergence has been found to be quick irrespective of the initial guess for the temperature profile.

The temperature distribution for different wall-to-wall optical thicknesses, κ_D, are obtained and plotted against the exact analytical results in Fig. 2. The net heat flux on the right wall is given by

$$q_2 = \pi\left(\bar{i}_{L,2} - \frac{\sigma T_2^4}{\pi}\right) \approx \pi\left(i_{L,e,2} - \frac{\sigma T_2^4}{\pi}\right) \tag{4}$$

where subscript 2 stands for the right wall. The agree-

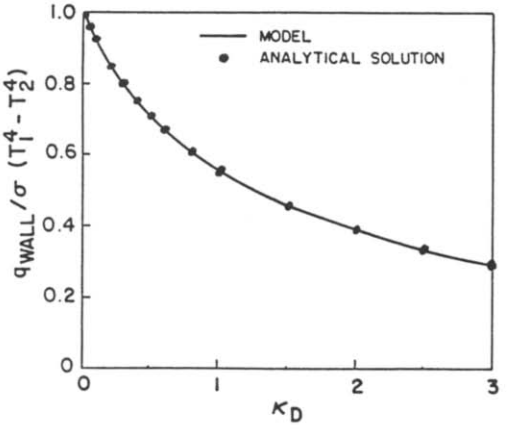

FIG. 3. Net radiative heat flux at the right wall for stagnant gray gas between black walls.

ment with the analytical solution (Fig. 3) within 0.1% validates the model for a non-isothermal gray medium. In these calculations, the walls have been assumed black at temperatures of 2000 and 1000 K, and 100 divisions per optical length were used for evaluating intensity.

Slot burner

A two-dimensional planar burner with the configuration depicted in Fig. 4 is chosen for the test case. A turbulent diffusion flame is established when methane, at 400 K, flows into the burner through the central duct at a velocity of 1 m s^{-1}, while air, also at 400 K, flows through the surrounding ducts at 3 m s^{-1}. The wall temperature is assumed constant at 400 K. As the surrounding velocity is higher than the central velocity, there is no recirculation region in the flow and the governing equation can be parabolized. The time averaged momentum, energy, and coupled species continually equations are solved using a modified version of GENMIX [19]. A one-step reaction with infinite rate chemical kinetics is assumed. A k–ε turbulence model is employed and radiation is completely neglected. The simplifications in the chemistry and turbulence calculations are justified, since one only needs a representative flow field to evaluate the radiation model. Conclusions drawn regarding the accuracy of the effective angle model from this study will be directly applicable to more sophisticated hydrodynamic numerical codes as well.

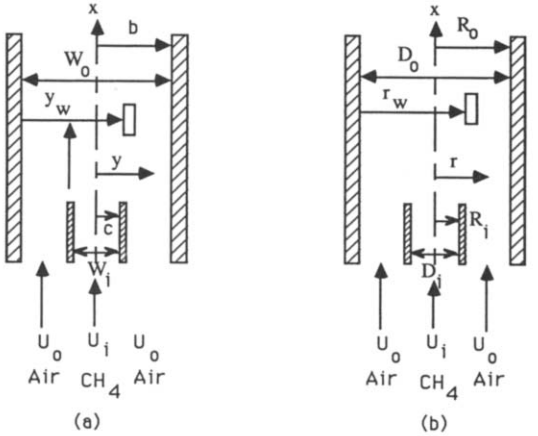

FIG. 4. Configurations of (a) model slot burner ($b = 1$ m, $c = 0.23$ m, $u_i = 1$ m s^{-1}, $u_0 = 3$ m s^{-1}) and (b) model cylindrical burner ($R_0 = 1$ m, $R_i = 0.4$ m, $u_i = 1$ m s^{-1}, $u_0 = 2$ m s^{-1}).

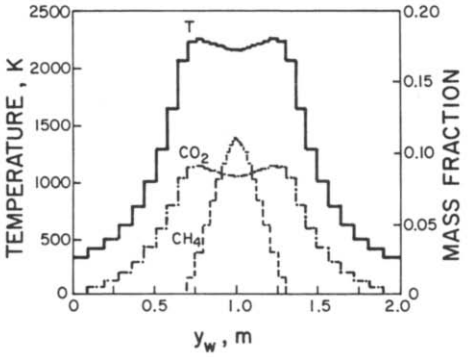

FIG. 5. Cross-stream variation of properties at $x/W_i = 25$ for the slot burner.

The computer program was run to generate and store the temperature and concentration of various radiating species throughout the flow. Typical cross-stream and downstream variations of properties are shown in Figs. 5 and 6. The concentration of water vapor can be obtained from that of CO_2 as they bear a fixed ratio. The axial temperature and product concentration increase till all the fuel is consumed, after which they decline due to cross-stream diffusion. The double peaks in the transverse profiles are associated with the two flame fronts.

Once the flow properties of the entire domain are stored, the TTNH model is employed to calculate the total intensity along any given line of sight. Any other intensity model could have been used, but this particular choice offered computational simplicity. The line of sight is divided into a number of discrete homo-

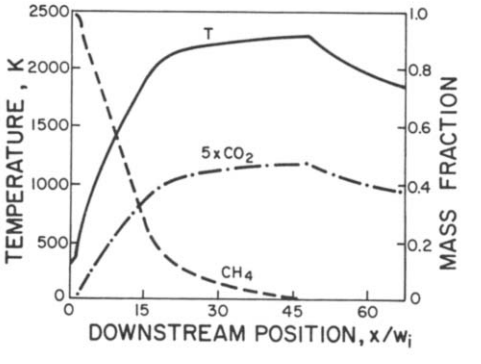

FIG. 6. Axial variation of temperature and various mass fractions in the slot burner.

geneous elements; the temperature and concentrations of various radiating species in each element are obtained by interpolation from the stored field. A data base called ABSORB [20] for the radiative properties of the species CO_2, H_2O, and CH_4 is used by TTNH to calculate the total intensity arriving at any given point in the flow from any given direction. Forty divisions of the longest line of sight were found sufficient for accurately representing the non-homogeneous profiles. In all the intensity calculations the walls have been considered black, which approximates many real combustion chambers in which the wall emissivity exceeds 0.9.

Once again referring to Fig. 1, the objective here is to see how accurately $i_{L,e}$ and $i_{R,e}$ describe the true averages $\bar{i}_L$ and $\bar{i}_R$ for any given element in the flow. The average intensity $\bar{i}_L$ can be evaluated from the total radiative heat flux incident on the left face of the element which is given by

$$q_L = \pi \bar{i}_L = \int_{2\pi} i'(\beta, \eta) \cos\beta \, d\omega$$

$$= 2 \int_{\eta=0}^{\pi} \int_{\beta=0}^{\pi/2} i'(\beta, \eta) \cos\beta \sin\beta \, d\beta \, d\eta. \quad (5)$$

Here, β is the angle between the line of sight and the y-direction, and η is the azimuthal angle. Twenty divisions in β and ten divisions in η were found more than adequate for accurate determination of the radiative flux. When the effective angle model is employed to estimate q_L, only one effective intensity needs to be computed as opposed to 200 intensities used for the precise determination of q_L from equation (5). In terms of the effective intensity, q_L is given by

$$q_L \approx \pi i_{L,e}. \quad (6)$$

The TTNH model is used as before to calculate this intensity along the pathlength $y_w/\cos 56°$. Properties in the y-direction at the location of interest are used instead of the interpolated properties along the actual line of sight.

The value of q_L calculated from equations (5) and (6) has been compared for various flow conditions at different locations in the combustor. Due to symmetry, it is sufficient to look only at the flux coming from the left, as q_R at any location (x, y) is exactly the same as q_L at $(x, -y)$. Figure 7 shows the comparison of q_L profiles obtained by the two methods at several downstream locations. The solid line represents full angular calculations in this and all subsequent plots. The value of q_L increases as one moves away from the relatively cool wall towards the hot flame zone, reaches a peak, and then decreases again due to absorption of radiation by the cooler layer of gas mixture near the right wall. The double peaks in the initial region indicate the presence of cooler fuel-rich gas mixtures near the burner center. The effective angle model, represented by the dashed lines can be seen to agree quite well with the full angular calculations. Only very close to the entrance region does one see some disagreement, which translates to a maximum error of 7% in the source term calculation. This is to be expected because of the drastic variation in properties along the axial direction near the entrance region. The radiative wall flux computed by the two methods is compared in Fig. 8 for two different chamber pressures. The characteristic optical thickness from the wall to the centerline increases from 0.1 to 2.0 (estimated with a characteristic temperature of 1700 K) as chamber pressure goes up from 0.1 to 5 atm. The temperature field remaining relatively unchanged as radiation was not coupled to hydrodynamics, the radiative flux level shows a marked increase at higher pressure. The model seems to perform as good or even better for optically thin media. This is also suggested by Fig. 9 where the calculations of Fig. 7 are repeated with a much lower chamber pressure of 0.1 atm.

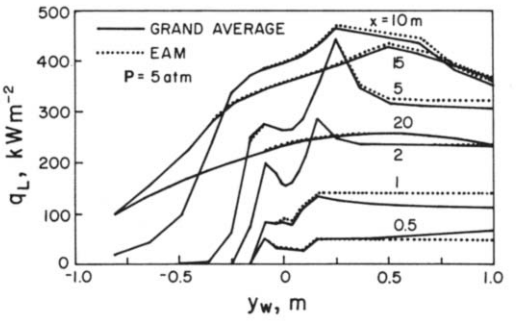

FIG. 7. Comparison of detailed calculation and EAM in the evaluation of q_L in the model parallel-plate burner.

The influence of other parameters including burner size and wall temperature have also been investigated and documented in ref. [21]. The model was found to be insensitive to a large variation in these parameters.

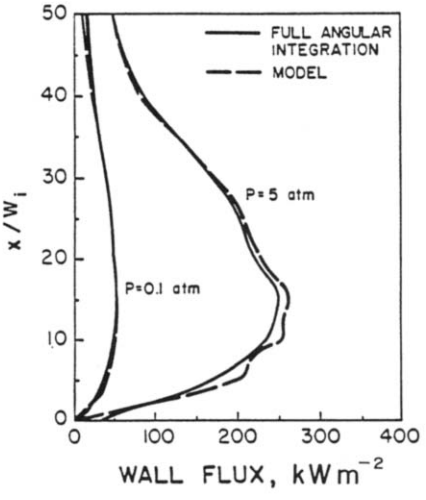

FIG. 8. Wall flux in the model parallel-plate burner for two different total pressures. Comparison of model with detailed calculations.

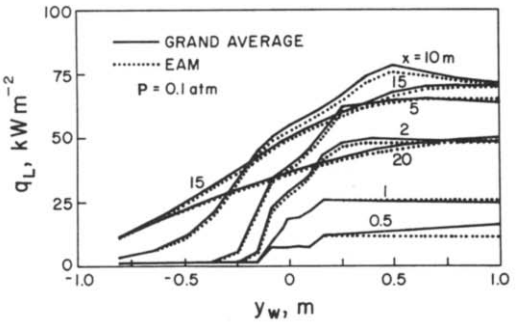

FIG. 9. Effect of optical thickness: calculation of Fig. 7 is repeated for an optically thin (low pressure) burner.

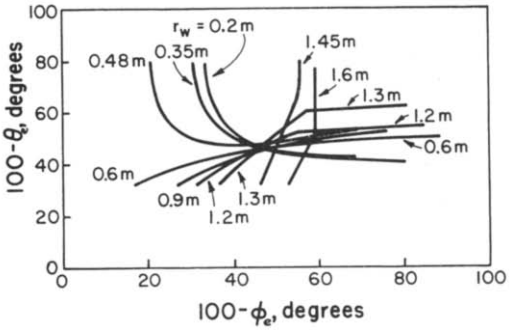

FIG. 11. Loci of (ϕ_e, θ_e) at different distances from wall (r_w values indicated in figure) at $x = 10$ m in the model cylindrical burner.

For example, when the burner width is reduced to $W_0 = 0.5$ m, the source term calculated by the two methods did not differ by more than 3% anywhere in the flow field.

MODEL FOR CYLINDRICAL ENCLOSURE

The extension of the effective angle model into cylindrical geometry is, by no means, a trivial matter. In evaluating the wall flux using the mean-beam-length model, Grosshandler [17] pointed out the difficulties associated with this geometry. With a slight change in the line of sight, there may be a striking variation of intensity.

Figure 10 shows a typical element in the cylindrical burner. Once again, one is interested in the radial flux incident on the right and left face of the element. The radiating enclosure to the left of the element, shown by the dotted region, lacks the symmetry of the planar geometry. The flux obtained from the mean-beam-length model will be an average over the surface enclosing the dotted region, and may be different from the flux at the location of interest, i.e. the left face of the element. In addition, the mean beam length of the enclosure will change with the radial location of the element. For example, for an element touching the axis, the mean beam length based upon the volume-to-area ratio is $1.23R_0$; when the element merges with the right wall, it equals $2R_0$. These complications make the prospect of a unique effective direction bleak. Nevertheless, the ultimate simplicity of the method makes it worthwhile to seek even an approximate effective direction in such a geometry.

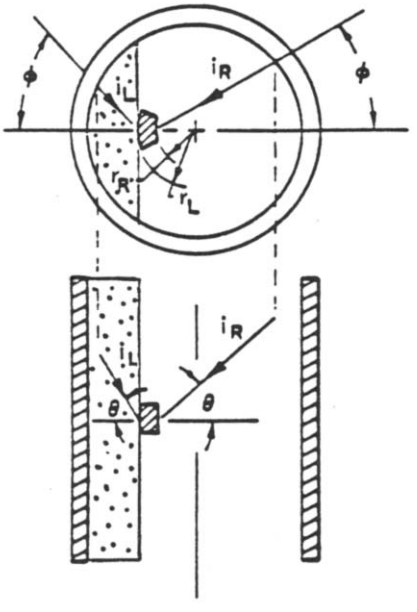

FIG. 10. Description of the line of sight in the cylindrical configuration.

In a manner similar to the procedure described in the case of the slot burner, the property field was generated and stored for the cylindrical burner depicted in Fig. 4. TTNH was employed to evaluate the intensity $i'(\phi, \theta)$ along any given line of sight. Note that two angles (ϕ, θ) are necessary for specifying the line of sight in cylindrical geometry (Fig. 10); they can be related to (β, η) through a geometric transformation. Equation (5) can be used to obtain the radiative flux incident on the left face of an element positioned anywhere in the flow. The task now is to seek out the effective directions (ϕ_e, θ_e) throughout the domain.

For any given location (x, r), 15 divisions each in ϕ and θ were found more than adequate for accurate evaluation of the heat flux q_L. As before, for computing the effective intensity at (x, r), properties at station x are extended in both axial directions to preserve the parabolic nature of the model. A systematic search is made for the whole range of ϕ and θ to determine the directions (ϕ_e, θ_e) for which

$$q_L = \pi \bar{i}_L = 2 \int_{\eta=0}^{\pi} \int_{\beta=0}^{\pi/2} i'(\beta, \eta) \cos\beta \sin\beta \, d\beta \, d\eta$$
$$\approx \pi i'(\phi_e, \theta_e). \quad (7)$$

For each (x, r) location, there may be a set of appropriate effective directions (ϕ_e, θ_e). The loci of such directions are plotted in Fig. 11 for a number of cross-

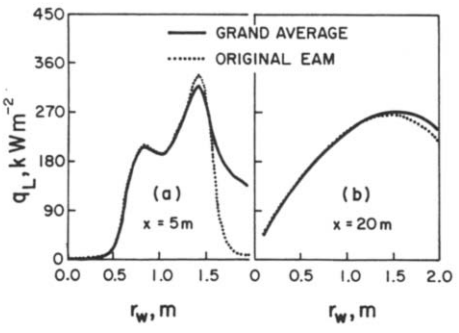

FIG. 12. q_L profiles evaluated by the crude EAM and detailed calculations at two downstream locations of the model cylindrical burner.

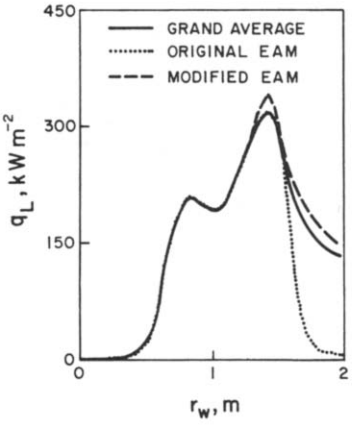

FIG. 14. q_L computed by exact, crude EAM, and modified EAM at $x = 5$ m in the model cylindrical burner.

stream positions at $x = 10$ m for the 2 m diameter burner. Except for locations close to the opposite wall ($r_w = 1.6$ m), almost all the loci intersect at a common point ($\phi_e = 45°$, $\theta_e = 45°$), indicating a possibility for a unique effective direction. When such calculations were repeated at many other downstream locations, very similar results were obtained. For stations far enough downstream where the cross-stream variation of properties becomes less steep, the loci intersect at about (45°, 45°) for all cross-stream locations. A very simplified effective angle model, $i_{L,e} = i'(45°, 45°)$, has thus emerged, which works almost everywhere except near the opposite wall in the initial region of the burner.

The failure of this empirical model in the initial region is illustrated in Fig. 12, where q_L, computed by the direct method and the model, are compared at $x = 5$ and 20 m locations. Except near the right wall at $x = 5$ m, there is good agreement between the model and the exact integration result. The reason for the discrepancy near the right wall can be understood with the help of Fig. 13, where a cross-section of the burner in the initial region is shown along with an element near the right wall. As the variation of properties in the r-direction is drastic in this initial region, it is possible for the flame to be surrounded by unreacted air. Neither heat nor any product of combustion (Lewis number is unity) has penetrated into the outer layer ($r > r_B$). Under such a circumstance, if the effective lines of sight completely lie in this cold outer portion, the model will be totally unaware of the presence of the flame and q_L will be underpredicted with a large error. This is exactly what is seen in Fig. 12 at $x = 5$ m for $r_w > 1.5$ m. Clearly, for locations up to point B (identified by the point of maximum radiative flux) of Fig. 13, no such problem arises. The effective angle model can, therefore, be assumed to be accurate till point B.

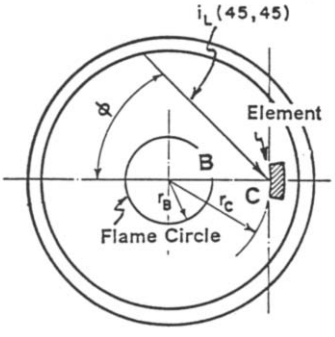

FIG. 13. A cross-section of the cylindrical burner showing the flame circle and a computational cell in the cold region.

A simple correction can be introduced for locations beyond the flame circle. The flux is assumed to be diminished primarily due to geometric considerations. For point C, then

$$q_{L,C} \approx q_{L,B} \frac{r_B}{r_C}. \tag{8}$$

The correction is unnecessary for far-downstream locations, where no such outer non-radiative layer exists due to sufficient mixing. A general correction formula is defined as follows:

$$q_L = \pi i_{L,e}(45°, 45°) \quad \text{for} \quad 0 < r_w < (R_o + r_B)$$

$$q_L = \max\left[\pi i_{L,e}(45°, 45°),\ q_{L,B}\frac{r_B}{r_C}\right] \quad \text{for} \quad (R_o + r_B) < r_w < 2R_o. \tag{9}$$

With this correction, the calculations of Fig. 12(a) are repeated and a much better agreement between the modified model and detailed calculations can be observed in Fig. 14.

It should be noted here that the choice of the effective angles is only approximate in nature. Because the intersection point of Fig. 11 extends over a finite zone, the results are not too sensitive to the choice of the effective angles. For a given application, the model can be 'fine-tuned' to improve accuracy.

TESTING THE CYLINDRICAL MODEL

Encouraged by the performance of the modified effective angle model in a specific case, the model has been tested in different burner conditions throughout the flow field. Comparison of the model with detailed calculations is shown in Fig. 15 at six downstream locations for the model cylindrical burner. The model is accurate within 1% beyond $x = 10$ m. For early regions, the error is higher, but acceptable, considering a 225-fold simplicity achieved by this model in comparison to the detailed calculations. Very similar behavior can be noticed for a smaller burner (Fig. 16) or for a burner with high wall temperature (Fig. 17).

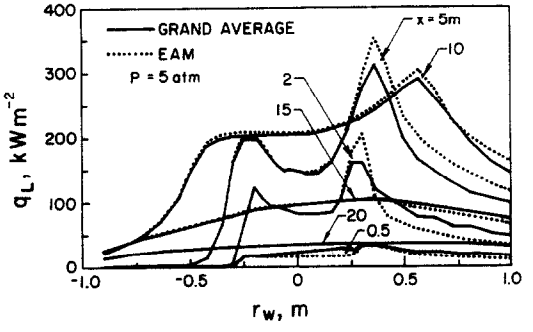

FIG. 15. EAM vs detailed calculations. q_L profiles at six different downstream locations in the model cylindrical burner.

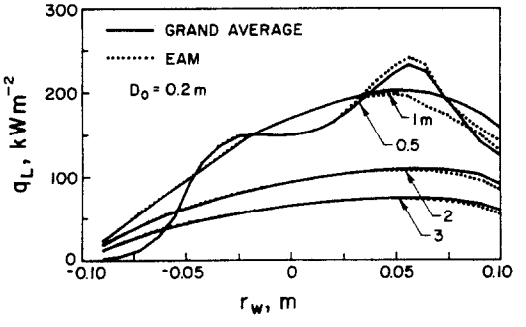

FIG. 16. Effect of burner size: q_L profiles at several downstream locations for a 0.2 m diameter burner.

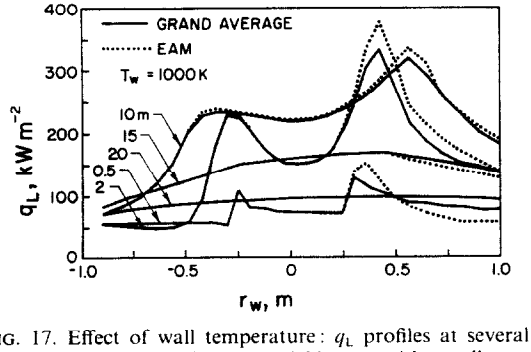

FIG. 17. Effect of wall temperature: q_L profiles at several downstream locations for the model burner with a wall temperature of 1000 K.

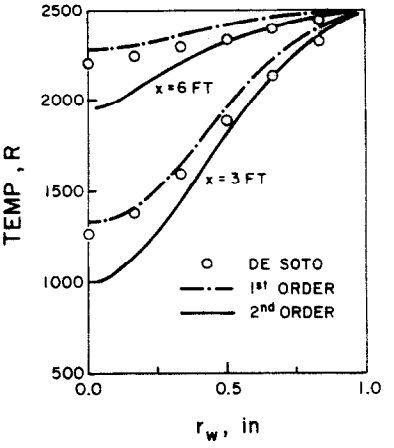

FIG. 18. Temperature profiles at $x = 3$ and 6 ft in a pipe of diameter 2 in. with a wall temperature of 2500 R. Comparison of de Soto's result with first- and second-order model.

In all these cases the model faithfully reproduced the peaks and valleys in the q_L profiles and is accurate within a few percent in most regions of the burner.

Although the model has been developed for the flow of combusting gases, where emission from the medium is the principal component of the radiative heat transfer, it has also been applied to the Graetz problem, where carbon dioxide flowing in the entrance region of a tube receives significant radiation from a high temperature wall. de Soto [22] produced a numerical solution for this case using a more accurate radiation model. His results are compared with the prediction using the effective angle model incorporated into GENMIX, shown in Fig. 18 as the second-order model. The first-order model also shown in the figure is based upon the thin gas approximation and is described elsewhere [23]. The first-order model slightly overestimates the radiation source term because it assumes that the energy from the hot wall penetration unattenuated to the center of the tube. The second-order model, on the other hand, apparently exaggerates the shielding effect and thus underpredicts the temperature in the central region. The discrepancy between de Soto's calculations and the second-order effective angle model may also be due to the different methods used to estimate the absorption coefficient for CO_2. At any rate, the combination of the TTNH model with the effective angle model makes the source term calculation so simple, that a sacrifice in accuracy can be justified under many circumstances.

NON-ISOTHERMAL BOUNDARY CONDITIONS

So far, the wall temperature of the burners has been assumed constant and known. In reality, however, the wall temperature will change with downstream position. Due to the parabolic nature of the

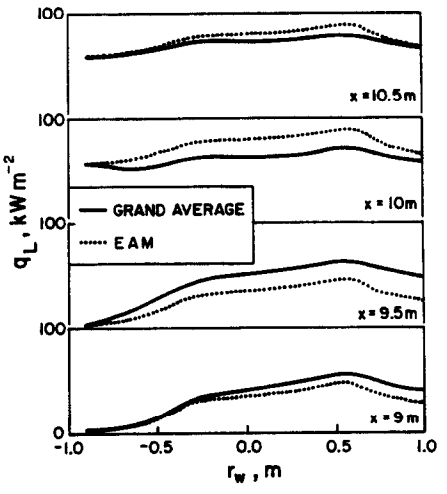

FIG. 19. q_L profiles at several locations around the step change in wall temperature (from 400 to 1000 K) at x = 9.75 m in the model cylindrical burner.

model, only the wall temperature at the current downstream location is used; as a result, the model will be unaware of any change in wall temperature away from the current location. How big a limitation does this impose on the model?

To address this question a large step change in wall temperature has been introduced in the boundary conditions of the model cylindrical burner. At $x = 9.75$ m the wall temperature is allowed to jump from 400 to 1000 K. Under this severe change in wall temperature, q_L is calculated using the model and the exact expression (equation (7)), and the results are compared in Fig. 19. The model underpredicts the radiative flux for locations before the step change as it does not take into account the contribution from the high temperature wall ahead of the current locations. For similar reasons it overestimates the radiative flux beyond $x = 9.75$ m. But the encouraging observation in this plot is the fact that the error in the model prediction quickly decreases on either side of the step change. For more gradual change in wall temperature, the error can be expected to be smaller, and to persist for an even shorter length. Therefore, the model can be applied to burners with adiabatic or any other type of boundary conditions without any catastrophic error. This model in burners with isothermal as well as adiabatic boundaries was used in coupling radiation to combustion chamber flows [23].

CONCLUSIONS

The effective angle model has been developed for evaluating the radiation source term in the confined flow of hot, radiating gas mixtures in rectangular and cylindrical geometries. While the mean-beam-length approach is used in the parallel plate configuration, an empirical trial-and-error method had to be used to determine the effective angles for the cylindrical configuration. The model reduces the problem of evaluating the radiation source term, at a given location in a flow to calculating two effective intensities arriving at that location from two effective lines of sight. For parallel plate geometry, the effective line of sight makes an angle $\beta_e = 56^\circ$ with the cross-stream (y) direction. When this model is applied to determine the temperature distribution in a stagnant gray gas in radiative equilibrium between two black parallel plates, satisfactory agreement with the analytical solution is obtained. For a combusting flow in a slot burner, the model results are compared with the detailed calculation of the exact expression for the radiative flux in the cross-stream direction. The model is accurate within a few percent for a wide variety of flow conditions.

In cylindrical geometry, the effective angles are $\phi_e = 45^\circ$, $\theta_e = 45^\circ$. A minor modification is needed in the initial flow region where there is a steep radial variation of properties. A similar comparison with the exact calculation is performed for various flow conditions. While the accuracy is lower in the cylindrical geometry, it is sufficiently high for most engineering applications. The model was also applied, with reasonable success, to the Graetz problem for a radiation absorbing gas in the entrance region of a tube. The model also showed satisfactory results when tested under a severe discontinuity in boundary temperature.

The primary advantage of the effective angle model is its simplicity. Only two intensities are needed to be computed for evaluating the radiation source term in any location of the flow field. The model is particularly useful for parabolic flows, for it does not disturb the marching nature of the solution procedure. Based on the properties of the current marching station, the effective intensities are evaluated at any cross-stream location where the radiation source term is desired.

Acknowledgement—This work has been supported by the National Science Foundation, grant number CBT-8412721.

REFERENCES

1. H. C. Hottel, *Heat Transmission* (Edited by W. H. McAdams) (3rd Edn). McGraw-Hill, New York (1954).
2. R. M. Goody, *Atmospheric Radiation I, Theoretical Basis*. Clarendon Press, Oxford (1964).
3. C. B. Ludwig, W. Malkmus, J. E. Reardon and J. A. Thompson, *Handbook of Infrared Radiation from Combustion Gases*, NASA SP-3080 (1973).
4. D. K. Edwards, L. K. Glassen, W. C. Hauser and J. S. Tuchscher, Radiation heat transfer in nonisothermal nongray gases, *J. Heat Transfer* **86**, 219 (1967).
5. J. D. Felske and C. L. Tien, Infrared radiation from nonhomogeneous gas mixtures having overlapping bands, *J. Quant. Spectrosc. Radiat. Transfer* **14**, 35 (1974).
6. T. H. Song and R. Viskanta, Development and application of a spectral group model to radiation heat transfer in a furnace, ASME Winter Annual Meeting, 86-WA/HT-36, Anaheim, December (1986).

7. W. L. Grosshandler, Radiative heat transfer in non-homogeneous gases: a simplified approach. *Int. J. Heat Mass Transfer* **23**, 1447–1459 (1980).
8. W. L. Grosshandler and A. T. Modak, Radiation from non-homogeneous combustion products. *Eighteenth Symp. (Int.) on Combustion*, pp. 601–609. The Combustion Institute, Pittsburgh (1980).
9. H. C. Hottel and A. F. Sarofim, *Radiative Heat Transfer*. McGraw-Hill, New York (1967).
10. A. Schuster, Radiation through a foggy atmosphere, *Astrophys. J.* **21**, 1–22 (1905).
11. S. Chandrashekhar, *Radiative Transfer*. Dover, New York (1960).
12. F. C. Lockwood and N. B. Shah, A new radiation solution method for incorporation in general combustion prediction procedure, *Eighteenth Symp. (Int.) on Combustion*, p. 1405. The Combustion Institute, Pittsburgh (1981).
13. J. M. Huang and J. D. Lin, Numerical analysis of Graetz problem with inclusion of radiation effect, National Heat Transfer Conf., Houston, Texas (1988).
14. R. Siegel and J. R. Howell, *Thermal Radiation Heat Transfer* (2nd Edn). Hemisphere, Washington, DC (1981).
15. B. E. Pearce and A. F. Emery, Heat transfer by thermal radiation and laminar forced convection to an absorbing fluid in the entry region of a pipe, *J. Heat Transfer* **92**, 221 (1970).
16. S. de Soto, Coupled radiation, conduction and convection in entrance region flow, *Int. J. Heat Mass Transfer* **11**, 39–53 (1968).
17. W. L. Grosshandler, Radiation from non-homogeneous mixtures in planar and cylindrical combustion systems, ASME/AIChE National Heat Transfer Conf., Orlando, Florida, 27–30 July, ASME, 80-HT-43 (1980).
18. M. A. Heaslet and R. F. Warming, Radiative transport and wall temperature slip in an absorbing planar medium, *Int. J. Heat Mass Transfer* **8**, 979–994 (1965).
19. D. B. Spalding, *GENMIX: A General Computer Program for Two-dimensional Parabolic Phenomena*. Paragon Press, Oxford (1977).
20. A. T. Modak, Radiation from products of combustion, *Fire Research* **1**, 339 (1979).
21. S. Bhattacharjee, Two-way radiation coupling in parabolic combusting flows, Ph.D. dissertation, Washington State University (1988).
22. S. de Soto, Coupled radiation, conduction and convection in entrance region flow, *Int. J. Heat Mass Transfer* **11**, 39–53 (1968).
23. S. Bhattacharjee and W. L. Grosshandler, Effect of radiation heat transfer on combustion chamber flows, *Combustion Flame* **77**, 347–357 (1989).

UN MODELE SIMPLIFIE DU TERME DE SOURCE RADIATIVE DANS LES ECOULEMENTS DE COMBUSTION

Résumé—On propose un "modèle d'angle effectif" pour évaluer le terme de source radiative dans les milieux non isothermes absorbants/émissifs, confinés dans des canaux rectangulaires et cylindriques. Tandis que le modèle possède la simplicité des schémas à deux flux, il incorporé l'influence de la géométrie du confinement et il est particulièrement adapté aux écoulements paraboliques car le terme source est basé sur les propriétés de la procédure choisie. Le modèle d'abord développé pour une géométrie bidimensionnelle, et appliqué au cas-type d'un milieu gris, reproduit des résultats analytiques à quelques pour cent. Il est ensuite appliqué à un brûleur plat bidimensionnel fonctionnant au fioul, en tenant compte des produits de combustion, et on compare favorablement les résultats avec un calcul détaillé du terme source. Avec une modification, le modèle est étendu à un brûleur cylindrique à gaz. Une étude des différents paramètres et conditions aux limites montre l'intérêt de ce modèle.

EIN VEREINFACHTES MODELL FÜR DEN STRAHLUNGSQUELLTERM IN BRENNENDEN STRÖMUNGEN

Zusammenfassung—Ein Modell für den "Wirkungswinkel" bei der Auswertung des Strahlungsquellterms in nicht-isothermen absorbierenden/emittierenden Strömungen in rechteckigen und zylindrischen Kanälen wird vorgestellt. Obwohl das Modell die Einfachheit des Zweistromprinzips aufweist, beinhaltet es den Einfluß der Hohlraumgeometrie und ist besonders geeignet für parabolische Strömungen, da der Quellterm auf den jeweils aktuellen Eignschaften während der Lösungsprozedur beruht. Das Modell wird zunächst für zweidimensionale Geometrien entwickelt und auf den Testfall eines grauen Strahlers angewandt, wobei eine Genauigkeit innerhalb einiger weniger Prozent erreicht wird. Danach wird es auf einen zweidimensionalen Schnittbrenner mit Strahlung vom Brennstoff und von bestimmten Verbrennungsprodukten angewandt. Das Ergebnis stimmt recht gut mit detaillierten Berechnungen überein. Das Modell wird mit einigen Änderungen auf einen zylindrischen Gasbrenner ausgeweitet. Eine Untersuchung mit veränderten Parametern und verschiedenen Randbedingungen unterstreicht die Vorzüge des Modells.

УПРОЩЕННАЯ МОДЕЛЬ, ОПИСЫВАЮЩАЯ ИСТОЧНИК ИЗЛУЧЕНИЯ В ГОРЯЩИХ ПОТОКАХ

Аннотация—Предложена "эффективная угловая модель" для оценки источника излучения в потоках неизотермических поглощающих/излучающих сред в прямоугольных и цилиндрических каналах. Обладая простотой двухпоточных схем, модель учитывает также влияние геометрии полости и является наиболее применимой для параболичнских течений, так как член, характеяизующий источник, базируется на характеристиках текущей координаты в процессе решения. В первую очередь модель разработана для двумерной геометрии и применялась в опыте с оптически серой средой, соответствуя аналитическим результатам с точностью до нескольких процентов. В дальнейшем она применялась для двумерной щелевой горелки с излучением от топлива и продуктов горения, и было показано удовлетворительное согласование с точными расчетами источника излучения. С некоторыми изменениями модель распространяется для случая цилиндрической газовой горелки. Изучение различных параметров и других типов граничных условий показывает перспективность модели.